A New Player in the Spermiogenesis Pathway of *Caenorhabditis elegans*

Craig W. LaMunyon,[1] Ubaydah Nasri, Nicholas G. Sullivan, Misa A. Shaw, Gaurav Prajapati, Matthew Christensen, Daniel Elmatari, and Jessica N. Clark
Department of Biological Science, California State Polytechnic University, Pomona, California 91768

ABSTRACT Precise timing of sperm activation ensures the greatest likelihood of fertilization. Precision in *Caenorhabditis elegans* sperm activation is ensured by external signaling, which induces the spherical spermatid to reorganize and extend a pseudopod for motility. Spermatid activation, also called spermiogenesis, is prevented from occurring prematurely by the activity of SPE-6 and perhaps other proteins, termed "the brake model." Here, we identify the *spe-47* gene from the *hc198* mutation that causes premature spermiogenesis. The mutation was isolated in a suppressor screen of *spe-27(it132ts)*, which normally renders worms sterile, due to defective transduction of the activation signal. In a *spe-27(+)* background, *spe-47(hc198)* causes a temperature-sensitive reduction of fertility, and in addition to premature spermiogenesis, many mutant sperm fail to activate altogether. The *hc198* mutation is semidominant, inducing a more severe loss of fertility than do null alleles generated by CRISPR-associated protein 9 (Cas9) technology. The *hc198* mutation affects an major sperm protein (MSP) domain, altering a conserved amino acid residue in a β-strand that mediates MSP–MSP dimerization. Both N- and C-terminal SPE-47 reporters associate with the forming fibrous body (FB)-membranous organelle, a specialized sperm organelle that packages MSP and other components during spermatogenesis. Once the FB is fully formed, the SPE-47 reporters dissociate and disappear. SPE-47 reporter localization is not altered by either the *hc198* mutation or a C-terminal truncation deleting the MSP domain. The disappearance of SPE-47 reporters prior to the formation of spermatids requires a reevaluation of the brake model for prevention of premature spermatid activation.

KEYWORDS spermatogenesis; spermiogenesis; fibrous body-membranous organelle; MSP

In most species, only a minute fraction of the total sperm produced succeeds in fertilizing an oocyte and passing a genome to the next generation. Upon entering the competition to fertilize an oocyte, the sperm must first transition from an immotile state to a state of active motility, and the timing of this transition is critical. Premature activation wastes stored energy reserves, while delayed activation allows competitors a head start in the race to the ova. In *Caenorhabditis elegans*, sperm activation occurs simultaneously with the final stage of sperm development: the transformation of the spherical spermatid into a crawling spermatozoon. Also called spermiogenesis, this wholesale cellular reorganization occurs rapidly and without the input of new gene products. This conversion is induced by two semiautonomous pathways. One pathway is male specific and is signaled by the extracellular protease TRY-5, which is thought to interact with SNF-10 on the sperm to initiate activation (Smith and Stanfield 2011; Fenker *et al.* 2014). The present study stems from a pathway operating in both males and hermaphrodites and involving the *spe-8* group gene products in signal transduction. Extracellular zinc can activate sperm via this pathway (Liu *et al.* 2013), but it is not known if it is the primary signal or if it acts at a later step in the pathway. Once internalized, both activation signals induce an influx of cations (Nelson and Ward 1980), a brief elevation in pH (Ward *et al.* 1983), the release of intracellular Ca^{2+} (L'Hernault 1997; Bandyopadhyay *et al.* 2002; Washington and Ward 2006), induction of a MAPK cascade (Liu *et al.* 2014), polymerization of major sperm protein (MSP), and fusion of the membranous organelles (MOs) with the plasma membrane (L'Hernault 1997).

While we are only beginning to learn the details of the TRY-5 activation pathway (Fenker *et al.* 2014), the *spe-8* group activation pathway has received much attention. This signal is transduced through SPE-8 (Muhlrad 2001; Muhlrad *et al.* 2014),

doi: 10.1534/genetics.115.181172
Manuscript received July 26, 2015; accepted for publication September 1, 2015; published Early Online September 2, 2015.
[1]Corresponding author: Department of Biological Sciences, California State Polytechnic University, 3801 W. Temple Ave., Pomona, CA 91768. E-mail: cwlamunyon@cpp.edu

SPE-12 (Shakes and Ward 1989; Nance *et al.* 1999), SPE-19 (Geldziler *et al.* 2005), SPE-27 (Minniti *et al.* 1996), and SPE-29 (Nance *et al.* 2000). Mutations in the encoding genes result in sperm that cannot activate in response to extracellular zinc (Liu *et al.* 2013), rendering hermaphrodites self-sterile although male mutants retain fertility through TRY-5 activation.

A suppressor screen of *spe-27(it132ts)* designed to identify additional members of the SPE-8 pathway turned up numerous mutations that suppress *spe-27* mutant sterility (Muhlrad and Ward 2002). Interestingly, none of the *spe-27* suppressors characterized so far are members of the SPE-8 group activation pathway. Instead, they bypass the need for an external activation signal altogether by causing premature sperm activation. Three genes harboring suppressor mutations have been identified, the first being *spe-6* (Muhlrad and Ward 2002). SPE-6, a predicted casein kinase, was known to function at earlier stages in spermatogenesis to package MSP into the fibrous body-membranous organelle complexes (FB-MOs) (Varkey *et al.* 1993). MSP forms the cytoskeleton for the sperm pseudopod and is segregated to the daughter cells during the meiotic divisions by way of the FB-MOs (Roberts *et al.* 1986). A surprisingly large number of suppressor mutations in *spe-6* were recovered. Because these mutations were spread across the coding sequence (CDS) and because many likely resulted in partial loss of function, SPE-6 was hypothesized to act as a "brake" on spermiogenesis, preventing spermatid activation until it was downregulated by the SPE-8 signaling pathway (Muhlrad and Ward 2002) or by the suppressor mutations.

Subsequently, suppressor mutations have been identified in *spe-4* (Gosney *et al.* 2008) and *spe-46* (Liau *et al.* 2013). SPE-4, a Presenilin-1 homolog, was also known to participate in FB-MO formation (L'Hernault and Arduengo 1992; Arduengo *et al.* 1998). Like the *spe-6* suppressors, the suppressor mutation in *spe-4* was hypomorphic (Gosney *et al.* 2008). The *spe-46* suppressor mutation also turned out to be hypomorphic, and in addition to premature sperm activation, it causes numerous sperm defects, including aneuploidy (Liau *et al.* 2013). While no null allele currently exists for *spe-46*, genetic analysis shows more severe loss of function results in sterility. The interpretation for the three genes identified by *spe-27* suppressor mutations is that they have two functions: (i) assembly of cellular complexes within developing spermatocytes and their proper segregation to the haploid spermatids and (ii) brake function, preventing sperm activation until reception of the activation signal. Here, we report on *spe-47*, a fourth gene discovered through a *spe-27* suppressor mutation. *spe-47(hc198)* is a mutation that causes premature spermatid activation, but SPE-47 protein is not found in spermatids, prompting a reevaluation of the brake protein hypothesis.

Materials and Methods

Worm strains and handling

All *C. elegans* strains were maintained on *Escherichia coli* OP50-seeded nematode growth media (NGM) agar plates and manipulated as described by Brenner (1974). The *Caenorhabditis* Genetic Center kindly provided the following strains: N2, CB4856, BA963: *spe-27(it132ts) IV*, BA966: *spe-27(it132ts) unc-22(e66) IV*, BA959: *spe-29(it129) dpy-20(e1282ts) IV*, BA786: *spe-8(hc53) I*, BA783: *spe-12(hc76) I*, BA959: *spe-29(it127) dpy-20(e1282) IV*, GR1373: *eri-1(mg366) IV*, DR466: *him-5(e1490) V*, BA17: *fem-1(hc17ts) IV*, JK654: *fem-3(q23ts) IV*, and EG5767: *qqIr7 I*; *oxSi78 II*; *unc-119(ed3) III*. The following strain was graciously provided by Steve L'Hernault: *spe-19(eb52) V*. The strain bearing the *hc198* mutation was isolated in a suppressor screen of *spe-27(it132ts)*; *unc-22(e66)* (Muhlrad 2001) (Muhlrad and Ward 2002). We backcrossed the *hc198*; *spe-27(it132ts) unc-22(e66)* line six times with *spe-27(it132ts)*, each time recovering *unc-22* F_2 that were fertile at 25°. This backcross line was the source for all subsequent lines carrying *spe-47(hc198)*. All other strains described herein were created for the purpose of this study. In general, *spe-27(it132)* was identified by an Unc phenotype due to its linkage to the *unc-22(e66)* mutation. Brood size was measured by counting the progeny laid daily by hermaphrodites isolated in 35-mm Petri dishes. In some cases, the effect of mating on hermaphrodite fertility was assessed, in which case individual hermaphrodites were maintained with four males each.

SNP mapping of hc198

The *hc198* mutation was localized to chromosome I using the polymorphic strain CB4856, commonly referred to as the Hawaiian (HA) strain for its Hawaiian origin. First, we backcrossed *hc198*; *spe-27(it132ts) unc-22(e61)* into the HA strain six times and assessed SNPs on chromosomes I (snp_Y71G12A[2], pkP1052, and snp_F26B1[1]), II (pkP2107, pkP2071), III (pkP3096, pkP3060), and V (snp_Y61A9LA[1], pkP5097). After finding N2 DNA on chromosome I, SNP loci on this chromosome were assessed to better define the region containing *hc198* (Figure 1). Next, as we have done to map other genes (Liau *et al.* 2013), we conducted a bulk-SNP mapping cross following the protocol of Wicks *et al.* (2001). Briefly, we crossed *hc198*; *spe-27(it132ts) unc-22(e61)* to the HA strain and isolated 120 F_2 L4 worms at 25°. Of these, 27 were fertile *hc198* homozygotes. These fertile worms were combined for bulk DNA extraction, as were another 27 sterile F_2 worms chosen arbitrarily. Using the two DNA extracts, plus DNA extracted from N2 and from HA, SNPs were analyzed from within the interval identified by backcrossing (Figure 1). The results from this approach to SNP mapping are in the form of map ratios, where ratios near 1.0 indicate an unlinked state, and map ratios close to 0.0 indicate linkage (Wicks *et al.* 2001).

Sequencing and analysis of the hc198 genome

Genomic DNA was extracted from the *hc198*; *spe-27(it132ts) unc-22(e66)* strain using standard methods. Briefly, we froze ~0.5 ml of worms in 4 ml of TEN (20 mM Tris, 50 mM EDTA, 100 mM NaCl) and digested them for 0.5 hr at 60° in TEN plus 0.5% SDS and 0.1 mg/ml Proteinase K. The

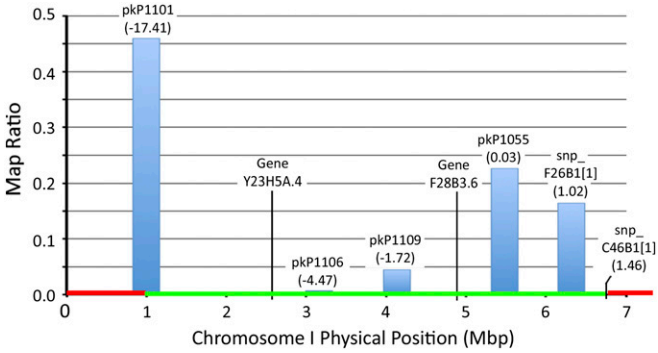

Figure 1 Mapping and localization of *hc198*. The map ratio is a measure of the linkage of *hc198* to SNPs on chromosome I. Map ratios near zero indicate linkage, whereas larger map ratios indicate greater distance to *hc198*. In addition, the green section of the *x*-axis surrounded by red indicates the region containing *hc198* after introgressing *hc198* into the polymorphic Hawaiian strain. Also shown are the two candidate genes harboring CDS altering mutations in the strain containing *hc198*.

concentration of Proteinase K was increased to 0.2 mg/ml, and the digestion was extended another hour. DNA was extracted from the digest via phenol/chloroform/isoamyl alcohol and precipitated with NaOAc/EtOH. The pellet was resuspended in TEN, RNase A was added to 40 mg/ml, and the digestion incubated for 1 hr. The DNA was extracted and precipitated as above and resuspended in TE. The DNA was transported to the City of Hope and Beckman Research Institute's DNA Sequencing/Solexa Core (Duarte, CA), where 80-bp reads from the ends of ~350-bp fragments of the DNA were sequenced using the Illumina Genome Analyzer II platform. The reads were mapped to chromosome I (accession no. NC_003279) using the bioinformatics software Geneious Pro.

Microinjection transformation for phenotypic rescue

Worms were transformed with PCR products from one of the two genes tested plus flanking sequence (Y23H5A.4 plus 1235 bp upstream and 787 bp downstream; F28B3.6 plus 1055 bp upstream and 579 bp downstream). The sequences were amplified from N2 DNA using the Expand High Fidelity^{PLUS} PCR System (Roche Diagnostics) following the manufacturer's protocols. The amplicons were purified using the Wizard SV Gel and PCR Clean-Up System (Promega). An injection mix of the PCR product (15 ng/μl) along with a plasmid containing P-*myo-3*::mCherry (pCFJ104, 100 ng/μl) was microinjected into the gonads of young adult *hc198*; *spe-27(it132ts)* hermaphrodites. Transformed worms were identified by mCherry fluorescence in the body wall muscle. F_2 transformants were checked for rescue (reduction in brood size), but transformed lines were not maintained past the rescue experiments because transgenes expressed in sperm are generally rendered ineffective by germline silencing after a small number of generations (Kelly and Fire 1998). For Y23H5A.4, we amplified the same sequence from *hc198* mutants for use as a negative control in transformation rescue.

RT-PCR

RNA was extracted from mixed age populations of worms from the strains *fem-1(hc17ts)* and *fem-3(q23ts)*. Large populations of each strain were collected and rinsed four times with M9 buffer. After freezing at −80°, the worms were disrupted by sonication in TRIzol reagent, and the RNA was extracted following the manufacturer's protocols (Life Technologies). The RNA samples were treated with RQ1 DNase (Promega) and subsequently purified via phenol-chloroform isoamyl alcohol extraction. RT-PCR was performed with the MyTaq One-Step RT-PCR kit (Bioline) per manufacturer's instructions. We multiplexed *spe-47*-specific primers (SeqF: 5′-GTTCTACTG GACCCTTTACG-3′ and Exon5R: 5′-TTGGAGCAGCGATGAGG TAG-3′) with primers specific to *act-2*, the *C. elegans* ortholog of β-actin (actinF: 5′-GTATGGGACAGAAAGACTCG-3′ and actinR: 5′-CGTCGTATTCTTGCTTGGAG-3′).

Construction of a spe-47 RNAi clone and induction of RNA interference

Using the MyTaq One-Step RT-PCR kit, a product was amplified from N2 RNA using primer pairs Y23-RNAiF and Y23-RNAiR (5′-actgCTCGAGgtttggacccttacg-3′ and 5′-cagtGCGGCCGCctcaccttcaaagc-3′, respectively). The primers were engineered with an added restriction site on the 5′ end for cloning: *Xho*I on the forward primer and *Not*I on the reverse primer (uppercase letters correspond to restriction enzyme sites; four bases were added to the 5′ end to maximize restriction enzyme activity). The amplicon was cloned into the pPD129.36 RNAi vector (Timmons *et al.* 2001) and transformed into *E. coli* HT115(DE3), a strain that lacks RNase III activity. Expression of double-stranded (dsRNA) from the insert was achieved through isopropyl-**β**-D-thiogalactopyranoside (IPTG) induction of T7 promoter sites flanking the pPD129.36 multiple cloning site.

Worms were exposed to the RNAi feeding strain bacteria in Petri dishes on agar prepared with 25 μg/ml carbenicillin and 1 mM IPTG. The plates were seeded with transformed HT115 bacteria that had been grown the previous night in a 2-ml liquid culture with LB media and 50 μg/ml carbenicillin and 15 μg/ml tetracycline. In the final hour of liquid culture, IPTG was added to a concentration of 1 mM. Large populations of worms were bleached (Stiernagle 1999) to obtain eggs, which were introduced onto the plates. At the L4 larval stage, exposed hermaphrodites were moved to their own RNAi plate, and their lifetime fecundity was measured. Identically handled control worms were exposed to HT115 bacteria containing the pPD129.36 empty vector.

CRISPR/Cas9 induced mutation of spe-47

To induce mutations likely to be molecular nulls, we utilized CRISPR-associated protein 9 (Cas9) technology (Friedland *et al.* 2013; Tzur *et al.* 2013). We created the single guide RNA (sgRNA) plasmid pCL45 by replacing the *unc-119* targeting site in the plasmid PU6::unc-119_sgRNA (Addgene) with a target site near the start of exon 4 on the opposite strand (5′-ggaagaaaaatacgccaaggAGG-3′). The target harbored

Table 1 Chromosome I nonsynonymous mutations in the *hc198* mapped region

Nucleotide position	Affected CDS	Mutation type	AA[a] change	*fem-3/fem-1*[b]	Expression[c]	Rescue fecundity[d]	Control fecundity[e]
2619128	*Y23H5A.4*	T to A	I to N	5.94	Spermatogenesis	11.2 ± 2.8 (16)	39.6 ± 3.8 (15)
4951466	*F28B3.6*	C to T	G to E	—	Muscle enriched	44.5 ± 7.7 (15)	48.2 ± 9.6 (14)

[a] AA, amino acid.
[b] Microarray data comparing sperm enriched (*fem-3*) to oocyte enriched (*fem-1*) mRNA (Reinke *et al.* 2000, 2004).
[c] Data from microarray studies as reported in WormBase (Harris *et al.* 2010).
[d] The fecundity ± SEM of *hc198*; *spe-27* mutant worms transformed with the wild-type copy of the gene. Sample size is in parentheses.
[e] The fecundity ± SEM of *hc198*; *spe-27* mutant nontransformed sibling worms as controls. Sample size is in parentheses.

a *Sty*I restriction site (underlined) next to the PAM sequence (uppercase, not included in targeting construct). The *Sty*I site allowed us to screen for small indels near the PAM sequence. We microinjected the sgRNA plasmid pCL45 and the Cas9-encoding plasmid Peft-3::cas9-SV40_NLS::tbb-2 at a concentration of 150 ng/μl each, along with the mCherry marker plasmids pCFJ104 (10 ng/μl), pCFJ90 (2 ng/μl), and pGH8 (5 ng/μl), which label the body wall muscles, the pharyngeal muscles, and neurons, respectively. We isolated F_1 worms that expressed the mCherry transformation markers and allowed them to produce populations. The F_1 populations were screened for mutations by extracting DNA from each, amplifying the region containing the CRISPR/Cas9 target site, and digesting the amplified products with *Sty*I following the same protocol used for SNP mapping (see section above). When a possible mutant F_1 population was identified, we isolated 24 worms from the population, and screened their progeny using the same protocol. We sequenced each mutation recovered. In addition, each CRISPR/Cas9 mutation was tested for its ability to suppress the *spe-27(it132ts)* sterile phenotype. We crossed male *spe-27 unc-22/spe-27* + with the CRISPR/Cas9 mutants and recovered F_2 that were phenotypically *unc-22*. If the CRISPR/Cas9 mutations suppressed *spe-27*, then 25% of the F_2 should have been fertile, which they were not.

Construction of spe-47 transcriptional and translational reporters

We created reporter constructs that were integrated into specific Mos1 sites following the Mos1-mediated Single Chromosomal Insertion (MosSCI) technique (Frokjaer-Jensen *et al.* 2008, 2012). First, we engineered a transcriptional fusion with GFP flanked by the *spe-47* promoter and 3′ UTR amplified from N2 DNA with Phusion High-Fidelity DNA polymerase (Thermo Scientific). The GFP coding sequence was amplified from the plasmid pPD95.75 (Addgene) with Phusion polymerase. The PCR primers were designed so that the products had regions of ~20 bp that overlapped, enabling us to stitch them together following the PCR fusion technique described by Hobert (2002). The transcriptional fusion was cloned into the multiple cloning site of the vector pCFJ151; the final construct contained 1235 bp upstream of the *spe-47* start codon (the next gene begins 846 bp upstream on the opposite strand), followed by the GFP coding sequence, and finally 851 bp downstream of the *spe-47* stop codon. The pCFJ151 vector targets the *ttTi5605* Mos1 insertion on chromosome II for homologous recombination.

We created three different translational fusions using the same general approach. The first was an N-terminal translational fusion with GFP, but here we combined the promoter, GFP (minus its stop codon), and the entire CDS plus 3′ UTR. These were stitched together and cloned into pCFJ151 as well to produce plasmid pCL30. A C-terminal translational fusion with mCherry was also constructed, combining the promoter plus entire CDS (minus its stop codon), the mCherry coding sequence (from plasmid pCFJ104), and the 3′ UTR. After PCR fusion, the construct was cloned into the vector pCFJ356 to create pCL43, which targets the *cxTi10816* Mos1 insertion on chromosome IV for homologous recombination. Finally, we used the Q5 Site-Directed Mutagenesis kit (New England BioLabs) to introduce the *hc198* mutation into pCL43 to create pGP1. The presence of the *hc198* mutation was confirmed by sequencing. We followed the MosSCI protocol to recover a homozygous integrated copy of each construct (Frokjaer-Jensen *et al.* 2008, 2012).

Microscopy, in vitro sperm activation, and microinjection transformation

Imaging was accomplished on a Nikon Eclipse Ti inverted microscope outfitted for Nomarski DIC and epifluorescence. All worms were dissected in SM1 buffer (Machaca *et al.* 1996), and nuclear material was labeled with 30 ng/μl Hoechst 33342 in SM1. Sperm were activated *in vitro* by exposure to SM1 containing 200 μg/ml pronase. Images were captured on a Nikon DS-Qi1 12-bit monochrome camera and analyzed with Nikon NIS Elements software. Imaging of reporter constructs was kept constant across experiments to reduce error (*e.g.*, the same exposure was used for each fluorophore/fluorescent label). The same microscope system was used for microinjection of nucleic acids into the gonads of recipient young adult hermaphrodites.

Data availability

Plasmids and strains created in this study are available upon request.

Results

Identification of spe-47, the coding sequence altered by hc198

The *hc198* mutation was ultimately identified through whole genome sequencing, but its chromosomal position was

determined initially by single nucleotide polymorphism (SNP) mapping. Prior to SNP mapping, we knew *hc198* was not on chromosome IV because it segregated independently from *unc-22*, a chromosome IV locus. The X chromosome was also not a likely location because no sperm genes reside there (Reinke *et al.* 2000). First, we backcrossed the *hc198* mutation into the polymorphic HA strain CB4856 six times and positioned it in a region of N2 identity from the original mutant strain on chromosome I flanked by HA DNA from pkP1101 (chromosomal position 992,136 bp) to snp_C48B6[1] (6,897,519 bp). No DNA of N2 identity was found on chromosomes II, III, or V. Second, we used bulk SNP mapping (Wicks *et al.* 2001) to narrow the map region on chromosome I. Briefly, after crossing our *hc198* mutant strain to the polymorphic Hawaiian strain CB4856, pooled mutant and nonmutant F_2 were subjected to PCR/RFLP analysis for SNP loci on the left arm of chromosome I. We obtained a map ratio near zero at SNP pkP1106 (3,163,074 bp), indicating this SNP locus is in close proximity to the mutation (Figure 1).

To identify all mutated genes in the genome of the *hc198*; *spe-27(it132) unc-22(e66)* strain, its DNA was sequenced at the City of Hope and Beckman Research Institute on the Illumina Genome Analyzer II platform. The sequencing was performed on two flow-cell lanes with 80-bp paired-end reads, generating a total of 89,330,364 reads. Using the bioinformatics software Geneious Pro (version 5.6.2), 16.0% of the reads, or 14,299,925 reads, were mapped to chromosome I. This percentage corresponded closely to the fraction of the genome found on chromosome I (15.8%) and provided an average depth of 76 reads per base pair. We searched the chromosome I alignment for mutations that created nonsynonymous alterations to coding sequences and that were present in >80% of the reads. The SNPs were compared to those found on chromosome I in six other sequenced mutant genomes from the same mutagenesis (Liau *et al.* 2013). Shared mutations were omitted from consideration, as they could not be the unique mutation responsible for the *hc198* suppressor phenotype. Only two genes with novel mutations were found in the map region for *hc198*: Y23H5A.4 and F28B3.6 (Table 1 and Figure 1). Microarray data suggested that Y23H5A.4 is upregulated in sperm (Reinke *et al.* 2000, 2004), while transcriptome profiling showed that F28B3.6 is expressed in sperm (Ma *et al.* 2014) (Table 1).

To determine if either candidate gene harbored the *hc198* mutation, we performed transformation rescue. Rescue of the *hc198* mutation should reduce fertility in an *hc198*; *spe-27* double mutant because *hc198* suppresses *spe-27* sterility. We microinjected the gonads of *hc198*; *spe-27(it132)* hermaphrodites with PCR-amplified wild-type products of each gene along with their respective promoter (Y23H5A.4: 1235 bp; F28B3.6: 1055 bp) and downstream sequences (Y23H5A.4: 787 bp; F28B3.6: 579 bp). The F_1 transformants were selfed, and the progeny of the F_2 transformants were counted. Transformation with wild-type F28B3.6 did not alter fecundity compared to nontransformed controls ($t = -1.14$, $P = 0.264$; Table 1), whereas wild-type Y23H5A.4 resulted in a significant reduction in fertility ($t = 6.098$, $P < 0.001$; Table 1). These results suggest that Y23H5A.4 harbors *hc198*. To confirm these results, we repeated the rescue experiment but substituted the mutated copy of Y23H5A.4 amplified from the mutants. Transformants containing the mutated Y23H5A.4 sequence had the same fecundity (38.4 ± 5.59; $n = 7$) as did the controls (34.2 ± 3.47; $n = 14$; $t = 0.670$, $P = 0.511$), indicating that only the wild-type version of Y23H5A.4 rescues the *hc198* phenotype, confirming that *hc198* is a lesion in Y23H5A.4.

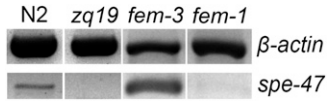

Figure 2 *spe-47* expression. A 573-bp region of *spe-47* cDNA was amplified in a multiplex reaction with a 954-bp segment of the cDNA of *act-2*, the *C. elegans* homolog of β-actin, as a control. Only a weak amplicon of *spe-47* was obtained from the wild-type strain N2, reflecting the brief period of spermatogenesis during hermaphrodite reproduction. A more prominent amplicon was amplified from *fem-3(q23)* hermaphrodites, which produce sperm for the duration of the adult hermaphrodite lifespan. Alternatively, no amplicon was found in *fem-1(hc17)* hermaphrodites, which never undergo spermatogenesis. No amplicon was obtained from *spe-47(zq19)* mutant worms. The *zq19* mutation induces a stop codon in exon 4.

The gene harboring *hc198* must be expressed in sperm, but the sperm expression of Y23H5A.4 was not entirely clear. Microarray studies indicated sperm expression (Reinke *et al.* 2004), while later transcriptome and proteome profiling did not (Ma *et al.* 2014). RT-PCR from *fem-3(q23)* mutant hermaphrodites (producing only sperm) amplified a prominent *spe-47* product, whereas only a very faint product was amplified from *fem-1(hc17)* mutant animals, which produce only oocytes (Figure 2). We also directed RNAi against a 573-bp segment of the Y23H5A.4 cDNA from exon 4 (amplified with primers Exon4F and Exon4R – see Figure 3). As for most sperm genes (del Castillo-Olivares *et al.* 2009), RNAi did not yield a sperm phenotype: the fecundity of RNAi exposed hermaphrodites was similar to that of control hermaphrodites exposed to bacteria containing the RNAi empty vector. (Figure 4; $F_{1,53} = 0.001$; $P = 0.974$). This was true for both the wild-type strain N2 and for the RNAi-sensitive strain *eri-1(mg366) IV* (Figure 4). In no case did we observe evidence of somatic phenotypes such as dumpy, uncoordinated, egg-laying defective, etc., supporting the sperm specificity of Y23H5A.4.

Henceforth we refer to Y23H5A.4 as the sperm gene *spe-47*. The SPE-47 protein comprises 380 amino acids, and the *spe-47(hc198)* mutation is a T-to-A transversion that substitutes asparagine for isoleucine at position 273, a nonpolar-to-polar change in the R-group (Figure 3A).

spe-47(hc198) has a spe phenotype on its own and bypasses the sperm activation pathway

The phenotype of the *spe-47(hc198)* mutation was investigated both as a suppressor of *spe-27(it132)* self-sterility and

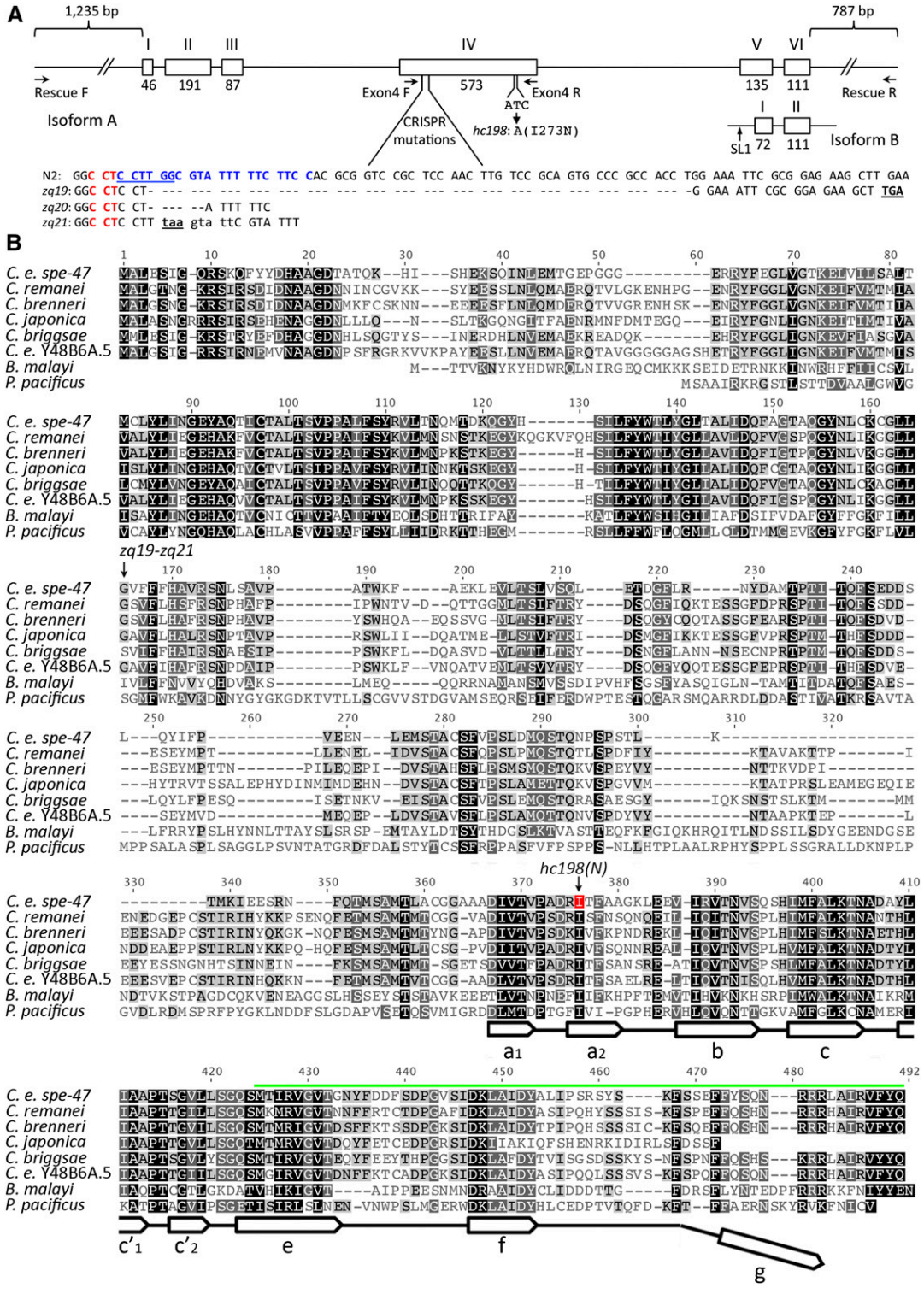

Figure 3 (A) Exonic structure of the two isoforms of *spe-47*. Shown are the locations of primers used to generate a rescuing PCR product and to produce an RNAi construct from exon 4. The locations of mutations are also shown, and the sequences of the CRISPR/Cas9 generated mutations are detailed below the gene structure. The guide RNA binding site (blue type) and PAM site (red type) are on the opposite strand and are thus shown in reverse complement. Premature stop codons induced by the CRISPR/Cas9 indels are in boldface type and underlined. The mutations do not affect isoform B, which has an SL1 leader sequence spliced onto the messenger RNA (mRNA) at the arrow. (B) Alignment of the SPE-47 protein sequence with orthologs and with the single *C. elegans* paralog. Darker background indicates greater conservation, and mutations are shown. Near the carboxy terminus a line with open arrows indicates the partial MSP domain, where the open arrows correspond to the seven β-strands based on *Ascaris suum* MSP-α. Note that the SPE-47 MSP domain is truncated at the carboxy terminus, missing the segment indicated by the downward bend in the MSP marker line. Also, the region encoded by isoform B is indicated by the green line.

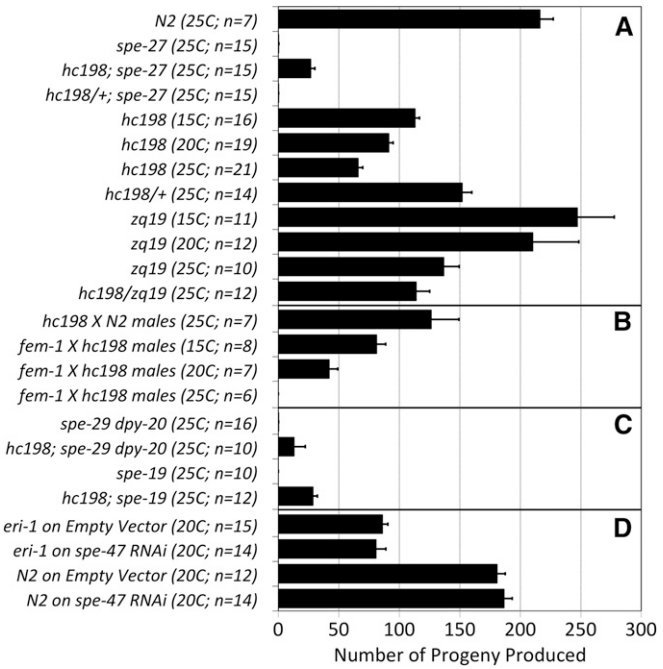

Figure 4 Fecundity associated with the various *spe-47* genotypes. (A) Hermaphrodite self-progeny showing that *spe-47(hc198)* is a recessive suppressor of *spe-27(it132)* sterility. In an otherwise wild-type background, selfing *spe-47(hc198)* hermaphrodites exhibit a temperature-sensitive spermatogenesis defect that is rescued by (B) mating with N2 males. Further in panel A, *spe-47(zq19)* causes a slight loss in fecundity but not as severe as does the *hc198* mutation at 25°. (B) Male *spe-47 (hc198)* mutant worms display a temperature-sensitive sperm defect when mating with spermless *fem-1(hc17ts)* hermaphrodites, being most fertile at 15° and sterile at 25°. (C) The *spe-47(hc198)* mutation suppresses mutations in both *spe-8* and in *spe-29*, restoring partial hermaphrodite self-fertility. Finally, (D) there is no effect of *spe-47* RNAi on the fertility of either wild-type worms or on RNAi-sensitive *eri-1(mg366)* worms. Error bars represent SEM.

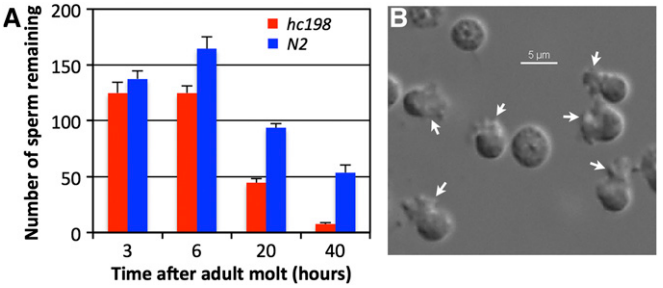

Figure 5 (A) Self-sperm remaining in hermaphrodites as a function of time since the adult molt. Error bars represent SEM. (B) Sperm dissected from a *spe-47(hc198)* mutant male. The arrows indicate pseudopods on prematurely activated spermatozoa. Wild-type males have only inactive spermatids.

as a Spe mutation in an otherwise wild-type background. Hermaphrodites homozygous for both *spe-47(hc198)* and *spe-27(it132ts)* produced a mean of 27 self-progeny at 25°. This *spe-27* suppression phenotype is recessive, as *spe-47(hc198)/+* hermaphrodites were sterile in a *spe-27* background (Figure 4A). In an otherwise wild-type background, *spe-47(hc198)* hermaphrodites exhibited a temperature-sensitive sperm defect: self-fertility dropped as temperature increased, and the fertility deficit was rescued when sperm was supplied by mating with wild-type males (Figure 4B). However, the *spe-47(hc198)* phenotype is semidominant in a wild-type background: heterozygous *spe-47(hc198)/+* hermaphrodites had greater self-fertility than homozygotes but less than N2 (Figure 4A).

We wondered if the low fertility of *spe-47(hc198)* hermaphrodites was due to a paucity of spermatids or to a problem with spermatid activation. We counted sperm nuclei observed in unmated mutant hermaphrodites at time intervals after the adult molt. Mutant hermaphrodites produced the same number of sperm as did wild type, but those sperm were lost rapidly with the onset of egg laying (Figure 5A). The same effect is seen in the *spe-8* group mutant hermaphrodites whose inactive spermatids are swept from the reproductive tract in early adulthood (L'Hernault *et al.* 1988). Unlike the *spe-8* group mutants, *spe-47(hc198)* self-fertility could not be rescued by exposure to male seminal fluid. This effect, termed transactivation (Nance *et al.* 2000), was assessed by combining L4 *spe-47(hc198)* hermaphrodites with L4 *fer-1(hc13)* males overnight at 25° in a ratio of 6 to 15, respectively, in 35-mm Petri dishes. When reared at 25°, *fer-1* males pass defective sperm to hermaphrodites, but their seminal fluid activates sperm from *spe-8* group mutant hermaphrodites (Shakes and Ward 1989). After isolating the mated *spe-47(hc198)* hermaphrodites, they produced a mean of only 4.8 progeny ($N = 12$; SEM = 1.1), which is similar to the 6.1 ($N = 12$; SEM = 1.0) progeny from control hermaphrodites not exposed to *fer-1* males. We then dissected *spe-47(hc198)* mutant hermaphrodites placed as L4 larvae at 25° the previous evening; under DIC microscopy, we found that 87.7% of their sperm were spermatids (65 sperm observed from 10 hermaphrodites), whereas only 10.5% of the sperm were in the spermatid stage in wild-type hermaphrodites under similar conditions (19 sperm observed from 11 hermaphrodites). Taken together, these results suggest that *spe-47(hc198)* hermaphrodites produce normal numbers of spermatids, of which a large proportion do not activate and are swept from the reproductive tract by passing eggs. Further, the defective sperm do not activate in response to TRY-5 protease delivered in the male seminal fluid.

Male *spe-47(hc198)* worms also suffer the fertility defect. When paired with spermless *fem-1(hc17)* hermaphrodites at 25°, *spe-47(hc198)* males sired no offspring, although they did produce cross-progeny at lower temperatures (Figure 4B), indicating that the male phenotype is also temperature sensitive. We dissected virgin *spe-47(hc198)* mutant males reared at 25° to examine the sperm stored within them and found that 28% were active spermatozoa. In total, 284 sperm were observed from eight males, and all males had active spermatozoa (Figure 5B). None of the sperm examined from comparable N2 male worms were active (166 sperm observed from four males). The presence of spermatozoa within virgin *spe-47(hc198)* males is likely the source of their infertility because crawling spermatozoa obstruct sperm transfer

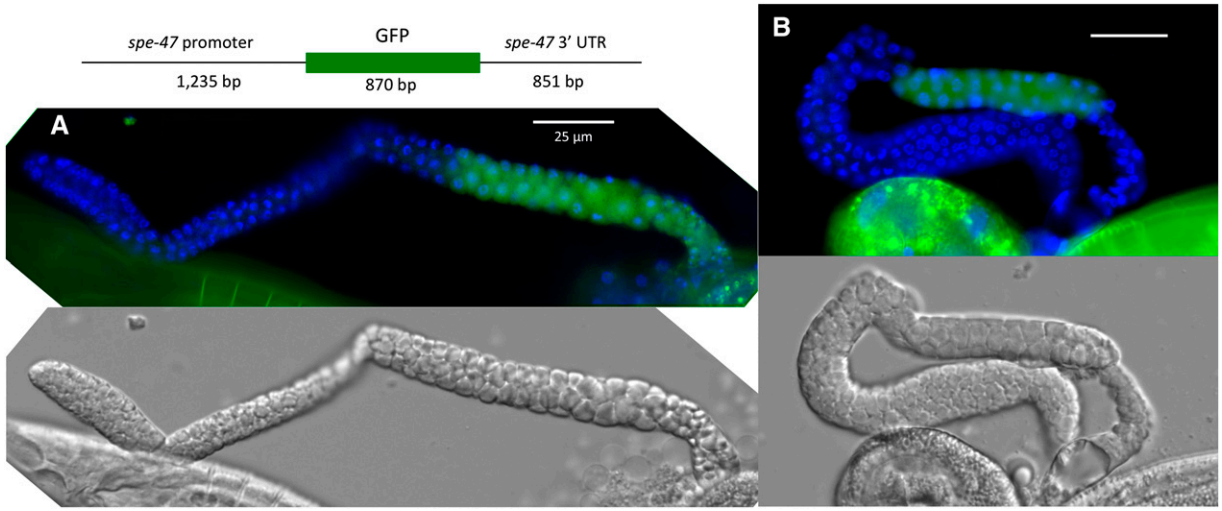

Figure 6 Expression of the *spe-47:GFP* transcriptional reporter. Here, the worms expressed an integrated GFP flanked by the *spe-46* promoter and 3′ UTR, and the tissue was labeled with the DNA dye Hoechst 33342. (A) In male gonads, GFP expression begins close to the end of the pachytene phase. (B) In gonads dissected from L4 hermaphrodites, GFP expression is evident in spermatogenic tissue at the same developmental stage as it is in the male gonad. Spermatogenesis proceeds from left to right in the regions of the gonads expressing GFP. Both bars, 25 µm.

during copulation (Stanfield and Villeneuve 2006). Surprisingly, the inactive spermatids in *spe-47(hc198)* males are capable of activation. We exposed the sperm to the proteolytic activity of the *in vitro* activator pronase (Ward *et al.* 1983) and found that 90% were active (of 129), which is similar to the 93% activation found in N2 (of 44). Collectively, these data suggest that *spe-47(hc198)* suppresses *spe-27(it132ts)* due to premature activation of a small number of spermatids, but that a large fraction fail to activate *in vivo*, although they may be activated *in vitro* by pronase.

It was previously shown that the *spe-27* suppressor alleles in *spe-4(hc196)*, *spe-6(hc163)*, and *spe-46(hc197)* restore fertility not only to *spe*-27 mutants but also to mutants of the other *spe-8* group genes (Muhlrad and Ward 2002; Gosney *et al.* 2008; Liau *et al.* 2013). The same is true for *spe-47(hc198)*: it suppressed the sterility of mutations in *spe-19* and *spe-29* (Figure 4C), demonstrating that its phenotype bypasses the need for the spermiogenesis activation pathway in a manner similar to the *spe-4*, *spe-6*, and *spe-46* suppressor alleles.

spe-47(hc198) is a semidominant mutation compared to CRISPR/Cas9 induced knockouts

Because we could not assess the severity of the *spe-47(hc198)* mutation on overall protein function, we created insertion/deletion mutations (indels) in *spe-47* using CRISPR/Cas9 technology (Friedland *et al.* 2013; Tzur *et al.* 2013). CRISPR/Cas9 employs both the Cas9 nuclease from *Streptococcus pyogenes* and a sgRNA containing a targeting sequence directed to the desired site in the genome. We designed the sgRNA to target a site near the beginning of exon 4 of *spe-47* (Figure 3A). Indels were predicted to disrupt a *Sty*I restriction site adjacent to the PAM sequence, allowing us to screen for potential mutants by PCR/restriction analysis (Friedland *et al.* 2013). We microinjected N2 worms with a plasmid containing the Cas9 nuclease sequence, plasmid pCL45 containing the sgRNA engineered to target *spe-47*, and plasmids to act as transformation markers. Three of 280 transformant F_1-derived populations had an altered restriction pattern, suggesting they harbored a mutation. Examination of 24 individuals from each potential mutant F_1 population confirmed the existence of the mutations and produced several homozygous populations. DNA sequencing revealed that the *zq19* mutation created a 56-bp deletion that causes a frameshift and a new stop codon after only six altered amino acids. The *zq20* mutation deletes 6 bp (two amino acids), and the *zq21* mutation is a 2-bp deletion replaced with an 8-bp insertion that encodes a stop codon (Figure 3A). Both *zq19* and *zq21* eliminate nearly 64% of the correct coding sequence. Further, RT-PCR from *spe-47(zq19)* mutants failed to amplify the *spe-47* transcript, suggesting that the induced premature stop codon results in destruction of the altered transcript via nonsense-mediated decay (Figure 2) and that *spe-47(zq19)* is a molecular null mutation.

Hermaphrodites homozygous for the *zq19* mutation produced 136.6 (SEM = 12.9, $N = 10$) offspring at 25°, a 37% reduction compared to wild type (Figure 4A), but *zq19* mutant fertility was greater than that of the *hc198* mutants (Figure 4A), providing further evidence that *hc198* is a semidominant mutation that has a more severe effect on fertility than a complete knockout of the gene. Surprisingly, the *zq19* mutation was conditional, with hermaphrodite fertility being greatest at 15° and lowest at 25° (Figure 4A), suggesting the SPE-47 may be involved in a process that is itself temperature sensitive. None of the CRISPR/Cas9 mutations suppressed *spe-27(it132ts)* sterility. We crossed each CRISPR/Cas9 mutant with *spe-27 unc-22* worms and recovered 15 F_2 worms that were *unc-22*. If the CRISPR/Cas9 mutations suppressed *spe-27* sterility, 25% of the F_2 should have been fertile, but none were fertile. Thus, none of the CRISPR/Cas9 mutations

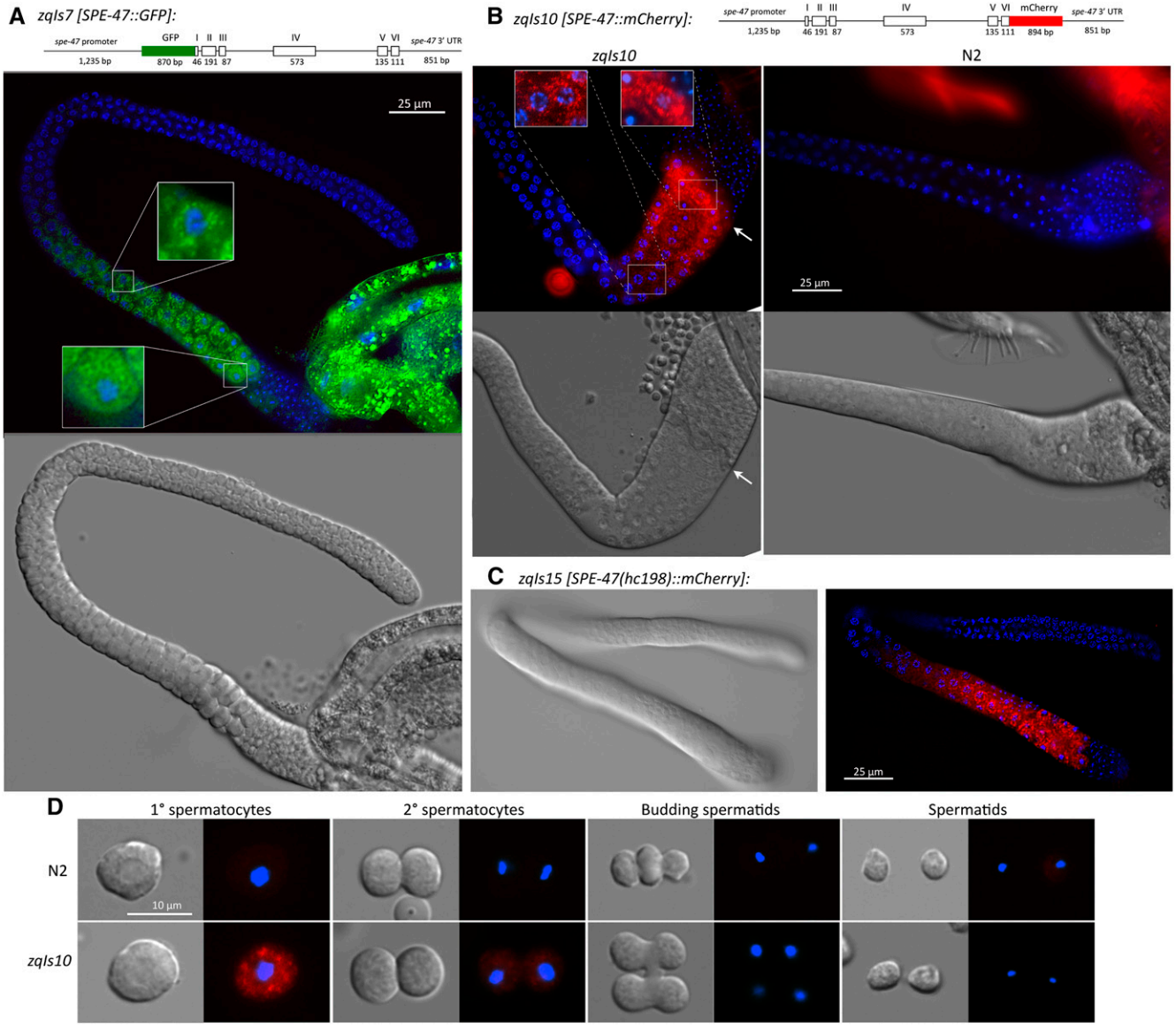

Figure 7 Localization of *spe-47* translational reporters. (A) GFP was fused to the N terminus of the *spe-47* coding sequence and integrated into a Mos1 site on chromosome II following the MosSCI technique. (B) A second reporter was constructed with mCherry fused to the C terminus of *spe-47*. The fluorescence of the reporter is shown next to a wild-type control. The expression of both reporters appears as puncta as the germ nuclei near the end of the pachytene phase. The fluorescence increases until the stage where the primary spermatocytes bud from the rachis (arrow), after which the fluorescence disappears. (C) The *spe-47*::*mCherry* reporter was altered to include the *hc198* mutation, and the localization of the mutated form appears identical to the wild type, with fluorescence appearing at the same stage and disappearing in the budding primary spermatocytes. (D) Examination of *spe-47*::*mCherry* fluorescence during the cellular stages of spermatogenesis. Fluorescence is clear in the cytoplasm of the primary spermatocytes, fades in the secondary spermatocytes, and is absent by the time spermatids bud from the residual body. In contrast, there is no fluorescence in wild-type controls (N2). Nuclei were labeled with Hoechst 33342.

suppressed *spe-27* sterility, further indicating that *hc198* is not a simple loss-of-function mutation. The fecundity of *hc198/zq19* transheterozygotes was 113.9 SEM = 11.2, $N = 12$), which is intermediate between the two homozygous strains (Figure 4A).

SPE-47 protein is conserved in nematodes and has an MSP domain

The *spe-47* gene has two isoforms (Figure 3A). Isoform A, the longer of the two, is the one mutated by *hc198*. The sequence of the protein encoded by isoform A contains a C-terminal MSP domain, and the sequence is conserved in other nematodes but not beyond. Alignment of the best BLAST matches from other *Caenorhabditis* species, from a putative paralog in *C. elegans*, and from the distantly related nematodes *Brugia malayi* and *Pristionchus pacificus*, indicates a high degree of conservation across much of the protein (Figure 3B). The *spe-47(hc198)* mutation not only alters an amino acid residue that is conserved across all species, it is a critical residue in the MSP domain (Figure 3B). MSP proteins contain an

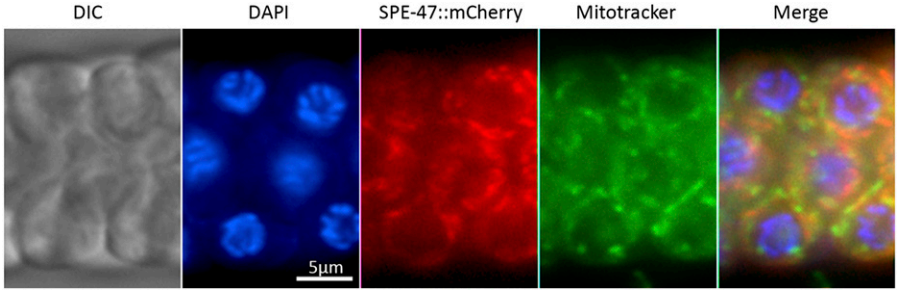

Figure 8 SPE-47::mCherry labeling does not overlap with MitoTracker Green FM in a region of an L4 hermaphrodite reproductive tract near the point where primary spermatocytes bud from the rachis.

immunoglobulin-like fold composed of seven β-strands (Figure 3B). Of these β-strands, the *a2* and *b* strands are critical to MSP dimerization (Smith and Ward 1998), so the fact that the *hc198* mutation disrupts a conserved residue in the *a2* strand strongly suggests that SPE-47 protein interacts with either MSP or with MSP domains on other proteins. Isoform B is the result of *cis*-splicing that introduces the SL1 *trans*-spliced leader at the 3′end of intron 4 of isoform A, an 850-bp intron (Figure 3A). Such *cis*-splicing is rare, but when it occurs, it is at the 3′ end of long introns (Allen *et al.* 2011). The protein encoded by isoform B is a truncated MSP domain (Figure 3). None of the mutations affect isoform B.

spe-47 localizes to FB-MOs early but disassociates and disappears during the first meiotic division

The location and timing of SPE-47 expression was investigated using transcriptional and translational reporter fusion constructs. We employed the MosSCI protocol (Frokjaer-Jensen *et al.* 2008, 2012) for single chromosomal insertions of reporter fusions to avoid the germline silencing encountered in expressing such constructs in extrachromosomal arrays. We first constructed a transcriptional reporter with GFP flanked by the sequences upstream and downstream of the *spe-47* coding sequence (Figure 6). GFP expression was localized to spermatogenic tissue, with expression initiating in midpachytene phase of meiosis I, and it was apparent in both male and hermaphrodite reproductive tracts (Figure 6).

We also examined subcellular localization with several translational fusions. One had GFP fused to the amino terminus (named *zqIs7*; Figure 7A), and another had mCherry fused to the carboxy terminus (named *zqIs10*; Figure 7B). Both reporters gave apparently identical patterns of fluorescence, which appeared in midpachytene, arising as circumnuclear puncta that became less distinct and larger as development proceeded. The fluorescence was most prominent in primary spermatocytes, faded in secondary spermatocytes, and was absent in budding spermatids (Figure 7D). Unfortunately, neither the N-terminal nor the C-terminal reporters rescued the *spe-47(hc198)* mutation. The N-terminal GFP fusion was tested with the strain ZQ122: *spe-47(hc198) I*; *zqIs7[spe-47::GFP] II*; *spe-27(it132ts) unc-22(e66) IV*. Rescue should result in sterility at 25°, but hermaphrodites produced a mean of 31.1 offspring (N = 15; SEM = 2.6). Control *spe-47(hc198) I*; *spe-27(it132ts) unc-22(e66) IV* lacking the *zqIs7* reporter actually produced fewer offspring, averaging 18.8 progeny (N = 15; SEM = 2.2). We tested the C-terminal fusion with the strain ZQ154: *spe-47(hc198) I*; *zqIs10[spe-47::mCherry] IV*; *spe-19(ok3428) V*. This strain produced 27.7 progeny (SEM = 3.7), a count that is similar to the fecundity of *spe-47(hc198) I*; *spe-19(ok3428) V* worms at 28.8 progeny (SEM = 3.8). Because the translational fusions failed to rescue *spe-47(hc198)* we cannot assert with certainty that the fusions accurately depict SPE-47 localization. However, we suggest that because all the translational fusions give strikingly similar patterns of fluorescence, it is likely that the observed pattern is correct.

The punctate localization suggests that the SPE-47 reporters associate with a cellular compartment. That compartment is not the mitochondria because SPE-47::mCherry did not overlap with MitoTracker Green FM (Life Technologies; Figure 8). Instead, the observed pattern of fluorescence bears striking resemblance to that of the FB-MOs during spermatogenesis (Kulkarni *et al.* 2012). We created a double reporter strain, combining SPE-47::mCherry with a PEEL-1::GFP translational reporter that labels the MOs (Seidel *et al.* 2011). Fluorescence from the two reporters overlaps in the early stage of expression, but the two appear separate by the stage at which the primary spermatocytes begin the first meiotic division (Figure 9), which is approximately the same stage at which they bud from the gonad rachis. Soon after, SPE-47::mCherry disappears while PEEL-1::GFP remains through the spermatid stage (Figure 9).

To better understand the localization of SPE-47::mCherry, we examined it in various mutant backgrounds. Mutant *spe-39(eb9)* worms do not form MOs but do produce FBs (Zhu and L'Hernault 2003), and localization appears unaltered in these mutants (Figure 10), indicating SPE-47 is not associated with MOs. In *spe-6* mutants, MOs form but FBs do not (Varkey *et al.* 1993). In a *spe-6(hc49)* mutant background, SPE-47::mCherry fluorescence is no longer punctate in the earliest stages of expression, although it does become typically punctate at the latest stages (Figure 10). Thus, the *spe-6(hc49)* mutation alters localization of the reporter fusion, suggesting that SPE-47 may interact with the FBs, at least in the early expression of SPE-47. Finally, we examined several alterations of our translational reporters. In one, we induced the *hc198* mutation in the SPE-47::mCherry reporter (named *zqIs15*), but the pattern of fluorescence appeared identical to that of the unmutated SPE-47::mCherry in both male gonads (Figure 7) and in hermaphrodite gonads (Figure 10). In

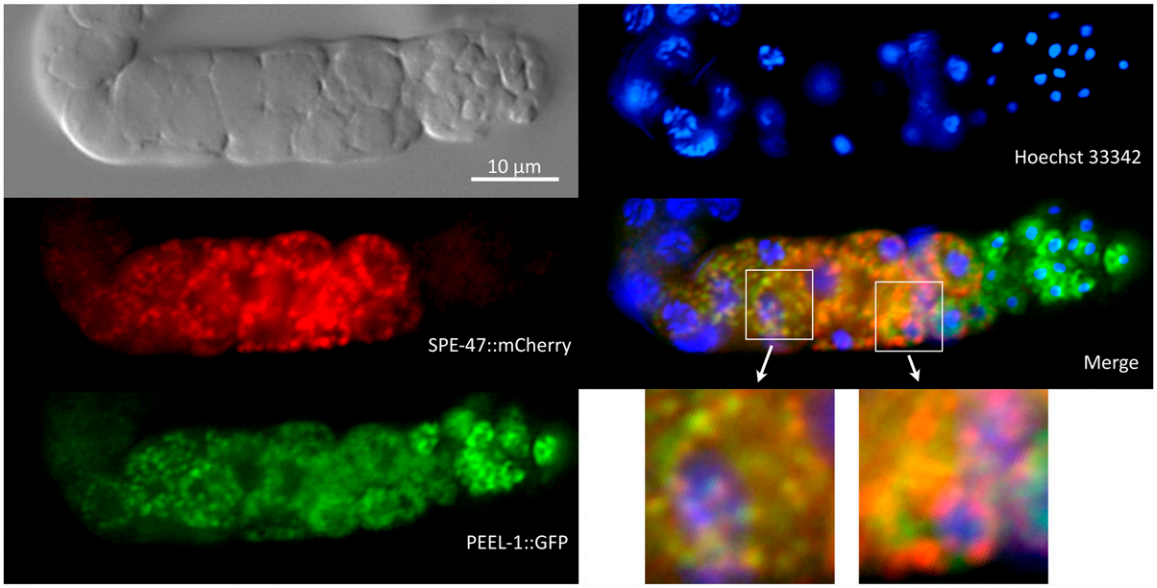

Figure 9 Colocalization of SPE-47::mCherry with MOs. Shown is an L4 hermaphrodite reproductive tract expressing both SPE-47::mCherry and PEEL-1::GFP, which labels the MOs. Both reporters appear at approximately the same stage, but SPE-47::mCherry disappears at the primary/secondary spermatocyte stage, while PEEL-1::GFP remains into the spermatids. The two reporters colocalize in the earliest stage of expression, but they appear distinct at the time when SPE-47::mCherry begins to disappear. Spermatogenesis proceeds from left to right.

another, we truncated the *spe-47* C-terminal coding sequence to remove the MSP domain and fused GFP in its place (named *zqIs5*), but again the pattern of fluorescence was unaltered (images not shown but similar to those in Figure 10).

Discussion

The *spe-47(hc198)* mutation was recovered as a recessive suppressor of *spe-27(it132ts)* sterility. Mapping and whole genome sequencing identified the mutated gene as *spe-47*, which has an MSP domain, but no other predicted features or similarity to proteins outside nematodes. We have shown that the *hc198* mutation is able to bypass the *spe-27(it132)* mutation—and the *spe-8* group signaling pathway—because it causes premature activation of a small fraction of sperm. Interestingly, in an otherwise wild-type background, *spe-47(hc198)* has a semidominant phenotype characterized by reduced brood size in hermaphrodites. Most of the mutant hermaphrodite sperm fail to activate and are swept from the reproductive tract by passing oocytes. Prematurely activated sperm are also found in *spe-47(hc198)* males. Surprisingly, the fraction of sperm not prematurely activated in males can be activated *in vitro* by exposure to the proteolytic activity of pronase, indicating that these sperm have a functional *spe-8* group activation pathway. Pronase cannot activate sperm with disrupted *spe-8* group signaling (Shakes and Ward 1989). However, the inactive sperm in *spe-47(hc198)* hermaphrodites are insensitive to TRY-5 in male seminal fluid, indicating that the TRY-5 activation pathway is compromised in *spe-47(hc198)* hermaphrodite sperm.

The *spe-27* suppressor mutations identified previously, *spe-4(hc196)*, *spe-6(hc163)*, and *spe-46(hc197)*, are also bypass suppressors with a small number of prematurely activated sperm accompanied by a large number of defective sperm (Muhlrad and Ward 2002; Gosney *et al.* 2008; Liau *et al.* 2013). According to the current model, these proteins act as a brake to activation, maintaining the spermatid stage until they are downregulated by the signal to activate (Muhlrad and Ward 2002). Results presented here call this model into question. Our SPE-47 reporter constructs disappear before spermatids are formed; if they localized correctly, these reporters indicate that the SPE-47 protein cannot inhibit activation because it is not present in spermatids.

Alternatively, at least some of the suppressor mutations may cause premature sperm activation by creating errors in sperm development, particularly as it relates to the FB-MOs. Under this hypothesis, proper formation and segregation of FB-MOs and perhaps other structures result in spermatids that undergo spermiogenesis only after receiving the extracellular signal to activate. We hypothesize that errors in this process lead to defective sperm, some of which activate prematurely and some of which do not activate at all. Prior to the budding of primary spermatocytes from the rachis, the FBs develop as MSP polymerizes into fibers within a cup-like membrane extension of the MO (Roberts *et al.* 1986). FB development is completed in primary spermatocytes, and FBs disassemble as the MSP depolymerizes within spermatids budding from the residual body, leaving only the MO in mature spermatids (L'Hernault 2006). FB formation is disrupted by null mutations in both *spe-4* and *spe-6* (L'Hernault and Arduengo 1992; Varkey *et al.* 1993; Arduengo *et al.* 1998), while the *spe-27* suppressor mutations in these genes are partial loss of function (Muhlrad and Ward 2002; Gosney *et al.* 2008), supporting the hypothesis that errors in FB-MO formation lead

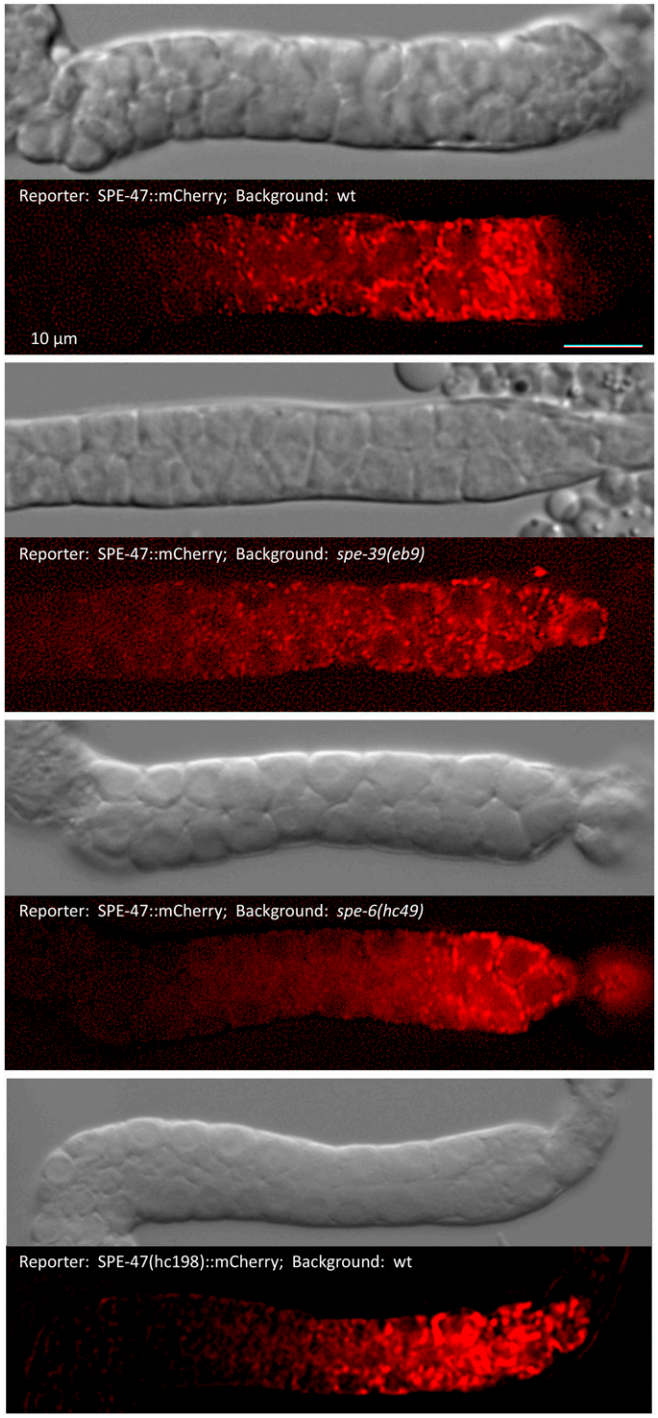

Figure 10 SPE-47::mCherry localization in various genetic backgrounds. Localization appears similar to wild type (wt) in a *spe-39(eb9)* mutant background. *spe-39* mutants make no MOs. Localization in the earliest stage of expression appears to be much less punctate in a *spe-6(hc49)* mutant background. *spe-6* null mutants such as *hc49* eliminate FB development. Finally, the localization of the SPE-47::mCherry reporter engineered with the *hc198* mutation appears unaltered compared to wild-type control. Spermatogenesis proceeds from left to right.

to defects such as premature activation. Similarly, defective segregation is seen in *spe-46(hc197)*, where aneuploid sperm are common. The *spe-47* results fit this hypothesis, as the SPE-47 reporters localize to the FB precisely as it is developing.

Given the fact that all the suppressor mutations found so far appear to support the hypothesis that errors in FB-MO formation cause premature sperm activation that bypasses the need for signaling through the SPE-8 group activation pathway, is there any remaining support for the brake protein hypothesis? We suggest that SPE-6 protein has a direct inhibitory function in addition to its role in FB formation as originally proposed by Muhlrad and Ward (2002). One of the most important facts supporting SPE-6 as a brake protein is that the original *spe-27* suppressor turned up ~25 alleles of *spe-6* (Muhlrad 2001; Muhlrad and Ward 2002), suggesting that simple loss of SPE-6 function causes premature sperm activation. The same screen identified only single alleles of *spe-4*, *spe-46*, and *spe-47*, suggesting that these mutations are not simply any routine loss of function but very specific alterations of function. The semidominant *hc198* mutation in *spe-47* is a good example of this. Finally, recent results show that SPE-6 is present in spermatids, existing as a halo around the nuclear material (D. Shakes and J. Peterson, personal communication), and that one *spe-6* mutation is an allele specific suppressor of *spe-27*, suggesting that the two proteins interact directly (our unpublished results). Thus, there appear to be two sources of inhibition to spermatid activation: SPE-6 protein and properly formed FB-MOs.

Our translational reporters suggest that SPE-47 protein associates with the FB-MO during its formation. It appears at approximately the same time that the FB-MOs begin to form and initially colocalizes with PEEL-1::GFP, an FB-MO label (Seidel *et al.* 2011). Further, early SPE-47::mCherry localization was disrupted in a mutant with no FBs (*spe-6* KO; Varkey *et al.* 1993) but was normal in a mutant with no MOs (*spe-39* KO; Zhu and L'Hernault 2003), suggesting that SPE-47 associates specifically with the FB. An FB role is reasonable, given that the FB is composed of MSP, and SPE-47 has an MSP domain. However, our truncated C-terminal SPE-47::GFP fusion localized normally even missing its MSP domain, so our hypothesized FB association must involve another domain in the protein. The importance of the MSP domain is demonstrated by the defective spermatids associated with the *hc198* mutation, which alters a β-strand known to be important to MSP–MSP dimerization (Smith and Ward 1998). Once the FB is fully developed, our SPE-47 reporters dissociate and disappear. We will test these hypotheses in future studies.

It is surprising that the CRISPR/Cas9 generated molecular null alleles of *spe-47* had only a very slight reduction in fertility, much less than that associated with the *hc198* mutation. We take this as further evidence that the *hc198* mutation is a very unusual alteration of function that results in a semidominant phenotype. However, this does not explain why the null alleles are nearly without a phenotype. A much reduced alternative isoform, *spe-47* isoform b, is expressed as a portion of the MSP domain. None of the mutations affect the isoform b, so it is conceivable that its expression moderates the effect of the isoform a mutations. In addition, a single paralog of

spe-47 exists in the *C. elegans* genome: Y48B6A.5. This gene has an MSP domain (Figure 3) and is upregulated in sperm. Thus, Y48B6A.5 and *spe-47* may have redundant functions, which would explain the lack of a more significant phenotype for the *spe-47* null alleles. In addition to investigating Y48B6A.5, we continue to study genes identified through the *spe-27(it132)* suppressor screen to gain a better understanding of sperm activation.

Acknowledgments

We are endebted to Paul Muhlrad, who originally isolated the hc198 mutation. We also thank Samuel Ward, who provided us with the large collection of spe-27 suppressor mutants. We are grateful to Steven L'Hernault, Paul Muhlrad, Diane Shakes, and Harold Smith for helpful discussions. This research was funded by National Institutes of Health (NIH) award 1SC3GM087212 and California State University Agricultural Research Institute award 10-4-179-33. Some strains were provided by the *Caenorhabditis* Genetics Center, which is funded by NIH Office of Research Infrastructure Programs (P40 OD010440).

Literature Cited

Allen, M. A., L. W. Hillier, R. H. Waterston, and T. Blumenthal, 2011 A global analysis of C. elegans trans-splicing. Genome Res. 21: 255–264.

Arduengo, P. M., O. K. Appleberry, P. Chuang, and S. W. L'Hernault, 1998 The presenilin protein family member SPE-4 localizes to an ER/Golgi derived organelle and is required for proper cytoplasmic partitioning during Caenorhabditis elegans spermatogenesis. J. Cell Sci. 111(Pt 24): 3645–3654.

Bandyopadhyay, J., J. Lee, J. Lee, J. I. Lee, J. R. Yu *et al.*, 2002 Calcineurin, a calcium/calmodulin-dependent protein phosphatase, is involved in movement, fertility, egg laying, and growth in Caenorhabditis elegans. Mol. Biol. Cell 13: 3281–3293.

Brenner, S., 1974 The genetics of *Caenorhabditis elegans*. Genetics 77: 71–94.

del Castillo-Olivares, A., M. Kulkarni, and H. E. Smith, 2009 Regulation of sperm gene expression by the GATA factor ELT-1. Dev. Biol. 333: 397–408.

Fenker, K. E., A. A. Hansen, C. A. Chong, M. C. Jud, B. A. Duffy *et al.*, 2014 SLC6 family transporter SNF-10 is required for protease-mediated activation of sperm motility in C. elegans. Dev. Biol. 393: 171–182.

Friedland, A. E., Y. B. Tzur, K. M. Esvelt, M. P. Colaiacovo, G. M. Church *et al.*, 2013 Heritable genome editing in C. elegans via a CRISPR-Cas9 system. Nat. Methods 10: 741–743.

Frokjaer-Jensen, C., M. W. Davis, C. E. Hopkins, B. J. Newman, J. M. Thummel *et al.*, 2008 Single-copy insertion of transgenes in Caenorhabditis elegans. Nat. Genet. 40: 1375–1383.

Frokjaer-Jensen, C., M. W. Davis, M. Ailion, and E. M. Jorgensen, 2012 Improved Mos1-mediated transgenesis in C. elegans. Nat. Methods 9: 117–118.

Geldziler, B., I. Chatterjee, and A. Singson, 2005 The genetic and molecular analysis of spe-19, a gene required for sperm activation in Caenorhabditis elegans. Dev. Biol. 283: 424–436.

Gosney, R., W. S. Liau, and C. W. Lamunyon, 2008 A novel function for the presenilin family member spe-4: inhibition of spermatid activation in Caenorhabditis elegans. BMC Dev. Biol. 8: 44.

Harris, T. W., I. Antoshechkin, T. Bieri, D. Blasiar, J. Chan *et al.*, 2010 WormBase: a comprehensive resource for nematode research. Nucleic Acids Res. 38: D463–D467.

Hobert, O., 2002 PCR fusion-based approach to create reporter gene constructs for expression analysis in transgenic C-elegans. Biotechniques 32: 728–730.

Kelly, W. G., and A. Fire, 1998 Chromatin silencing and the maintenance of a functional germline in Caenorhabditis elegans. Development 125: 2451–2456.

Kulkarni, M., D. C. Shakes, K. Guevel, and H. E. Smith, 2012 SPE-44 implements sperm cell fate. PLoS Genet. 8: e1002678.

L'Hernault, S. W., 1997 Spermatogenesis, pp. 271–294 in *C. elegans II*, edited by D. L. Riddle, T. Blumenthal, B. J. Meyer, and J. R. Priess. Cold Spring Harbor Laboratory Press, Cold Spring Harbor, NY.

L'Hernault, S. W., 2006 Spermatogenesis, pp. 1–14 in *WormBook*, ed. The *C. elegans* Research Community WormBook, http://www.wormbook.org.

L'Hernault, S. W., D. C. Shakes, and S. Ward, 1988 Developmental genetics of chromosome I spermatogenesis-defective mutants in the nematode *Caenorhabditis elegans*. Genetics 120: 435–452.

L'Hernault, S. W., and P. M. Arduengo, 1992 Mutation of a putative sperm membrane protein in Caenorhabditis elegans prevents sperm differentiation but not its associated meiotic divisions. J. Cell Biol. 119: 55–68.

Liau, W. S., U. Nasri, D. Elmatari, J. Rothman, and C. W. LaMunyon, 2013 Premature sperm activation and defective spermatogenesis caused by loss of spe-46 function in Caenorhabditis elegans. PLoS One 8: e57266.

Liu, Z., L. Chen, Y. Shang, P. Huang, and L. Miao, 2013 The micronutrient element zinc modulates sperm activation through the SPE-8 pathway in Caenorhabditis elegans. Development 140: 2103–2107.

Liu, Z., B. Wang, R. He, Y. Zhao, and L. Miao, 2014 Calcium signaling and the MAPK cascade are required for sperm activation in Caenorhabditis elegans. Biochim. Biophys. Acta 1843: 299–308.

Ma, X., Y. Zhu, C. Li, P. Xue, Y. Zhao *et al.*, 2014 Characterisation of Caenorhabditis elegans sperm transcriptome and proteome. BMC Genomics 15: 168.

Machaca, K., L. J. DeFelice, and S. W. L'Hernault, 1996 A novel chloride channel localizes to Caenorhabditis elegans spermatids and chloride channel blockers induce spermatid differentiation. Dev. Biol. 176: 1–16.

Minniti, A. N., C. Sadler, and S. Ward, 1996 Genetic and molecular analysis of *spe-27*, a gene required for spermiogenesis in *Caenorhabditis elegans* hermaphrodites. Genetics 143: 213–223.

Muhlrad, P. J., 2001 A genetic and molecular analysis of spermiogenesis initiation in *Caenorhabditis elegans*, in *Molecular and Cellular Biology*. Ph.D. Thesis, University of Arizona, Tucson.

Muhlrad, P. J., and S. Ward, 2002 Spermiogenesis initiation in *Caenorhabditis elegans* involves a casein kinase 1 ENCODED by the spe-6 gene. Genetics 161: 143–155.

Muhlrad, P. J., J. N. Clark, U. Nasri, N. G. Sullivan, and C. W. LaMunyon, 2014 SPE-8, a protein-tyrosine kinase, localizes to the spermatid cell membrane through interaction with other members of the SPE-8 group spermatid activation signaling pathway in C. elegans. BMC Genet. 15: 83.

Nance, J., A. N. Minniti, C. Sadler, and S. Ward, 1999 spe-12 encodes a sperm cell surface protein that promotes spermiogenesis in *Caenorhabditis elegans*. Genetics 152: 209–220.

Nance, J., E. B. Davis, and S. Ward, 2000 spe-29 encodes a small predicted membrane protein required for the initiation of sperm activation in *Caenorhabditis elegans*. Genetics 156: 1623–1633.

Nelson, G. A., and S. Ward, 1980 Vesicle fusion, pseudopod extension and amoeboid motility are induced in nematode spermatids by the ionophore monensin. Cell 19: 457–464.

Reinke, V., H. E. Smith, J. Nance, J. Wang, C. Van Doren *et al.*, 2000 A global profile of germline gene expression in C. elegans. Mol. Cell 6: 605–616.

Reinke, V., I. S. Gil, S. Ward, and K. Kazmer, 2004 Genome-wide germline-enriched and sex-biased expression profiles in Caenorhabditis elegans. Development 131: 311–323.

Roberts, T. M., F. M. Pavalko, and S. Ward, 1986 Membrane and cytoplasmic proteins are transported in the same organelle complex during nematode spermatogenesis. J. Cell Biol. 102: 1787–1796.

Seidel, H. S., M. Ailion, J. Li, A. van Oudenaarden, M. V. Rockman *et al.*, 2011 A novel sperm-delivered toxin causes late-stage embryo lethality and transmission ratio distortion in C. elegans. PLoS Biol. 9: e1001115.

Shakes, D. C., and S. Ward, 1989 Initiation of spermiogenesis in C. elegans: a pharmacological and genetic analysis. Dev. Biol. 134: 189–200.

Smith, H. E., and S. Ward, 1998 Identification of protein-protein interactions of the major sperm protein (MSP) of Caenorhabditis elegans. J. Mol. Biol. 279: 605–619.

Smith, J. R., and G. M. Stanfield, 2011 TRY-5 is a sperm-activating protease in Caenorhabditis elegans seminal fluid. PLoS Genet. 7: e1002375.

Stanfield, G. M., and A. M. Villeneuve, 2006 Regulation of sperm activation by SWM-1 is required for reproductive success of C. elegans males. Curr. Biol. 16: 252–263.

Stiernagle, T., 1999 Maintenance of *C. elegans*, pp. 51–67 in *C. elegans: A Practical Approach*, edited by Hope, I. Oxford University Press, Oxford.

Timmons, L., D. L. Court, and A. Fire, 2001 Ingestion of bacterially expressed dsRNAs can produce specific and potent genetic interference in Caenorhabditis elegans. Gene 263: 103–112.

Tzur, Y. B., A. E. Friedland, S. Nadarajan, G. M. Church, J. A. Calarco *et al.*, 2013 Heritable custom genomic modifications in *Caenorhabditis elegans* via a CRISPR-Cas9 system. Genetics 195: 1181–1185.

Varkey, J. P., P. L. Jansma, A. N. Minniti, and S. Ward, 1993 The *Caenorhabditis elegans spe-6* gene is required for major sperm protein assembly and shows second site non-complementation with an unlinked deficiency. Genetics 133: 79–86.

Ward, S., E. Hogan, and G. A. Nelson, 1983 The initiation of spermiogenesis in the nematode Caenorhabditis elegans. Dev. Biol. 98: 70–79.

Washington, N. L., and S. Ward, 2006 FER-1 regulates Ca2+-mediated membrane fusion during C. elegans spermatogenesis. J. Cell Sci. 119: 2552–2562.

Wicks, S. R., R. T. Yeh, W. R. Gish, R. H. Waterston, and R. H. Plasterk, 2001 Rapid gene mapping in *Caenorhabditis elegans* using a high density polymorphism map. Nat. Genet. 28: 160–164.

Zhu, G. D., and S. W. L'Hernault, 2003 The *Caenorhabditis elegans* spe-39 gene is required for intracellular membrane reorganization during spermatogenesis. Genetics 165: 145–157.

Communicating editor: B. Goldstein